Macromolecules
Cite This: Macromolecules 2019, 52, 700−707
Article
pubs.acs.org/Macromolecules

Thermally Activated One-Pot, Simultaneous Radical and Condensation Reactions Generate Surface-Anchored Network Layers from Common Polymers

C. K. Pandiyarajan[†] and Jan Genzer*[,†,‡]

[†]Department of Chemical & Biomolecular Engineering, North Carolina State University, Raleigh, North Carolina 27695-7905, United States

[‡]Global Station for Soft Matter, Global Institution for Collaborative Research and Education (GI-CoRE), Hokkaido University, Hokkaido 060-0808, Japan

Supporting Information

ABSTRACT: We present a versatile one-pot synthesis method that generates surface-attached polymer networks by cross-linking common polymers using thermally active 6-azidosulfonylhexyltriethoxysilane (6-ASHTES), which acts as a cross-linker and a surface-anchoring agent. We deposit a thin layer (∼200 nm) of a mixture comprising a given amount of 6-ASHTES and a polymer onto the substrate and anneal it at elevated temperatures (100−140 °C). Upon heating, the sulfonyl azide groups release nitrogen, and the resulting nitrenes abstract protons from the neighboring C−H bonds in polymers and undergo a C−H insertion reaction and/or recombination to form sulfonamide bonds. Condensation among ethoxysilane headgroups in bulk links 6-ASHTES units completes cross-linking. Simultaneously, 6-ASHTES reacts with substrate-bound −OH or C−H groups and attaches the covalently cross-linked polymer to the substrate. We carry out systematic investigation of gel kinetics involving annealing temperature, annealing time, and the concentration of 6-ASHTES for various polymer systems. This simple yet versatile approach involving simultaneous radical and condensation reactions adjusts the gel fraction in the polymer network and anchors the network to various substrates.

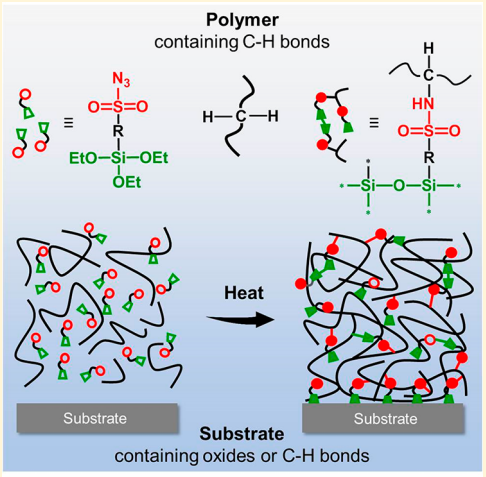

INTRODUCTION

Research in polymer thin films and functional coatings has gained considerable attention due to potential applications in many fields, including, electronics,[1] aviation,[2] medical devices,[3] tissue engineering,[4] microfluidics,[5] or marine technology,[6] just to name a few. Substrate-anchored polymer coatings have been conventionally generated by adopting either the grafting-to[7] or the grafting-from[8,9] strategies. Polymer networks on substrates have been formed by employing a precursor copolymer incorporating a cross-linkable unit, i.e., a photoactive (e.g., benzophenone) or thermally active (e.g., sulfonylazide) moieties, and grafting them to surfaces, which contain precoated anchoring chemical motifs.[10] Irradiation with UV-light or exposure to heat triggers the cross-linking and surface-attachment reactions, thus resulting in surface-anchored polymer networks. We have previously demonstrated that such an approach can be applied to a variety of surfaces, ranging from soft polymers to metals.[11−13] However, the general application of these methods is limited due to the complexity associated with synthesizing specialty macromolecules bearing cross-linker/anchoring motifs. In addition, all existing methods for generating surface-anchored polymer networks require at least two fabrication steps (i.e., cross-linking and immobilization).[14] Reducing the number of synthetic steps and implementing robust cross-linking and substrate anchoring reactions should make such systems more practical and appealing for many applications.[15−17] It also provides a cost-effective and robust means of fabricating commercial coatings.

Herein, we report a simple one-pot synthesis that generates surface-anchored polymer networks using thermally active 6-azidosulfonylhexyltriethoxysilane (6-ASHTES). The incorporation of sulfonyl azide (SAz) and triethoxysilane functionalities facilitates simultaneous cross-linking and surface attachment of the polymer network to the substrate. In a typical experiment, we mix a given amount of 6-ASHTES with the precursor polymer and deposit a film on the substrate by dip coating (cf. Figure 1a). We then expose the sample to an elevated temperature, which triggers cross-linking and concurrent attachment of the network to the substrate.[10]

Received: October 12, 2018
Revised: December 21, 2018
Published: January 8, 2019

DOI: 10.1021/acs.macromol.8b02194
Macromolecules 2019, 52, 700−707

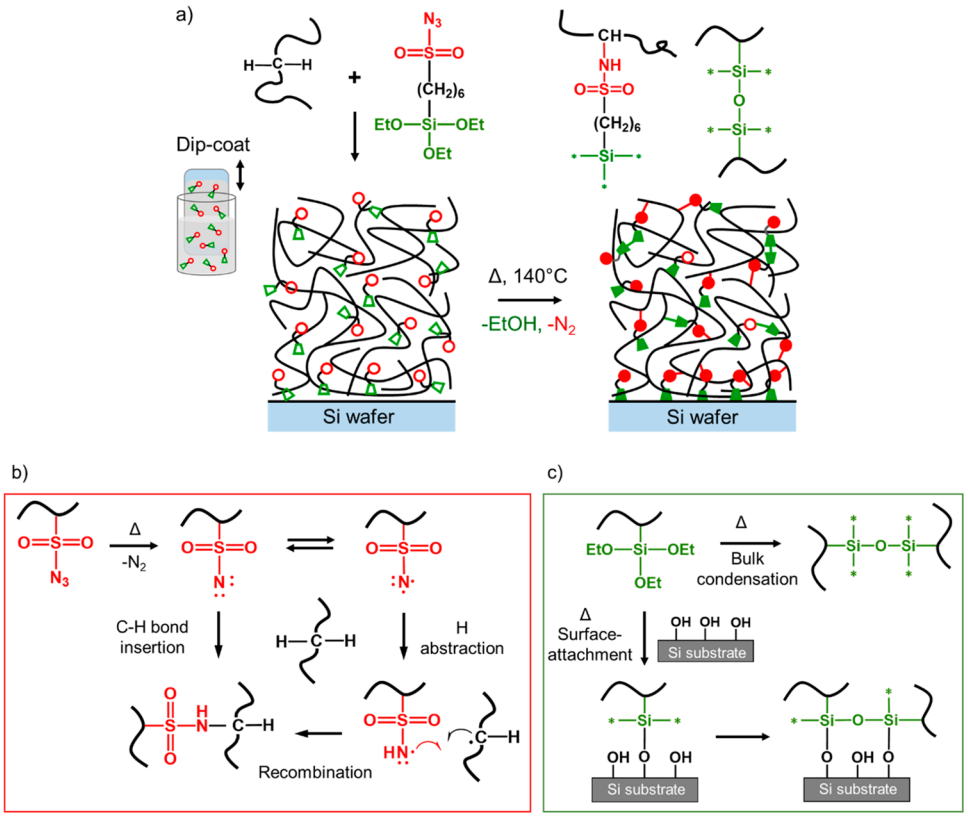

Figure 1. (a) Schematics of surface-attached network formation via one-pot synthesis, where the open and solid symbols indicate unreacted and reacted sulfonyl azide (red circle) and ethoxy (green trapezoid) groups in 6-ASHTES, respectively. Proposed reaction mechanism of (b) sulfonyl azide cross-linking and (c) surface-attachment of the 6-ASHTES.

Upon heating the sample to temperatures >100 °C, the azide groups release nitrogen gas and form singlet nitrenes, which are in equilibrium with the triplet state.[18] The active triplet abstracts a proton from a neighboring C−H bond leaving nitrogen and carbon radicals (cf. Figure 1b), which yields a sulfonamide bond.[19] The triethoxysilane groups in 6-ASHTES undergo condensation and form siloxanes linkage (*vide infra*), which complete the cross-linking process. Concurrently, 6-ASHTES molecules anchor the network to the substrate by condensation with surface hydroxyl groups (cf. Figure 1c).[20,21] This simple process leads to simultaneous network formation and immobilization on the substrate.

RESULTS

Thermal Cross-Linking of 6-ASHTES. We explored the aforementioned cross-linking scheme to (cf. Figure 1) generate surface-attached network films using a variety of polymer precursors. Figure 2 plots the gel fraction (P_{gel}) of poly(vinylpyrrolidone) (PVP) and poly(propargyl methacrylate) (PPGMA) as a function of 6-ASHTES concentration (cf. Figure 2a,b) and annealing temperature (cf. Figure 2c,d). All samples were annealed for 300 min. We determine P_{gel}, i.e., the insoluble fraction of polymer in the network, by dividing the polymer layer thickness (measured using spectroscopic ellipsometry; see the Supporting Information) before (d_0) and after (d) extraction of the cross-linked polymer film:[11]

$$P_{gel} = \frac{d}{d_0} \quad (1)$$

The data in Figure 2 indicate that P_{gel} depends on the amount of 6-ASHTES in the PVP/6-ASHTES mixture and chemical composition of the polymer after 300 min of annealing at a given temperature. In Figure 2a, P_{gel} increases with increasing 6-ASHTES concentration in the PVP/6-ASHTES mixture and annealing temperature. One can adjust simultaneously the concentration of 6-ASHTES and the annealing temperature to achieve a desired value of P_{gel}. For instance, networks with $P_{gel} \approx 0.65$ can be generated by using PVP/6-ASHTES mixtures with 6-ASHTES content equal to 5, 10, or 20 wt % and annealing them at 140, 130, or 120 °C, respectively (cf. Figure 2a). We also performed similar studies with PPGMA. In Figure 2b, we plot the dependence of P_{gel} of PPGMA network on wt % of 6-ASHTES. The PPGMA networks exhibit higher P_{gel} values for the same 6-ASHTES concentration and annealing temperature relative to the PVP networks. The dependence of P_{gel} on the concentration of 6-ASHTES and annealing temperature in PPGMA networks is the same as that in the PVP ones. We attribute the faster cross-linking kinetics in PPGMA relative to PVP to faster formation of sulfonamide bonds (*vide infra*). Such behavior, reported previously for benzophenone,[22,23] stems from the difference in the molecular structure of the respective polymers. The cross-linking reaction in PVP occurs primarily via the polymer backbone. In contrast, the methyl and methylene groups in the backbone and the side chain in PPGMA participate equally in the cross-linking reaction and hence lead to faster reaction and higher P_{gel}.[24]

We next replot P_{gel} for both PVP and PPGMA as a function of log(T), where we choose one of the data sets (i.e., 5 wt % of 6-ASHTES) arbitrarily as a benchmark and shift the remaining

DOI: 10.1021/acs.macromol.8b02194
Macromolecules 2019, 52, 700−707

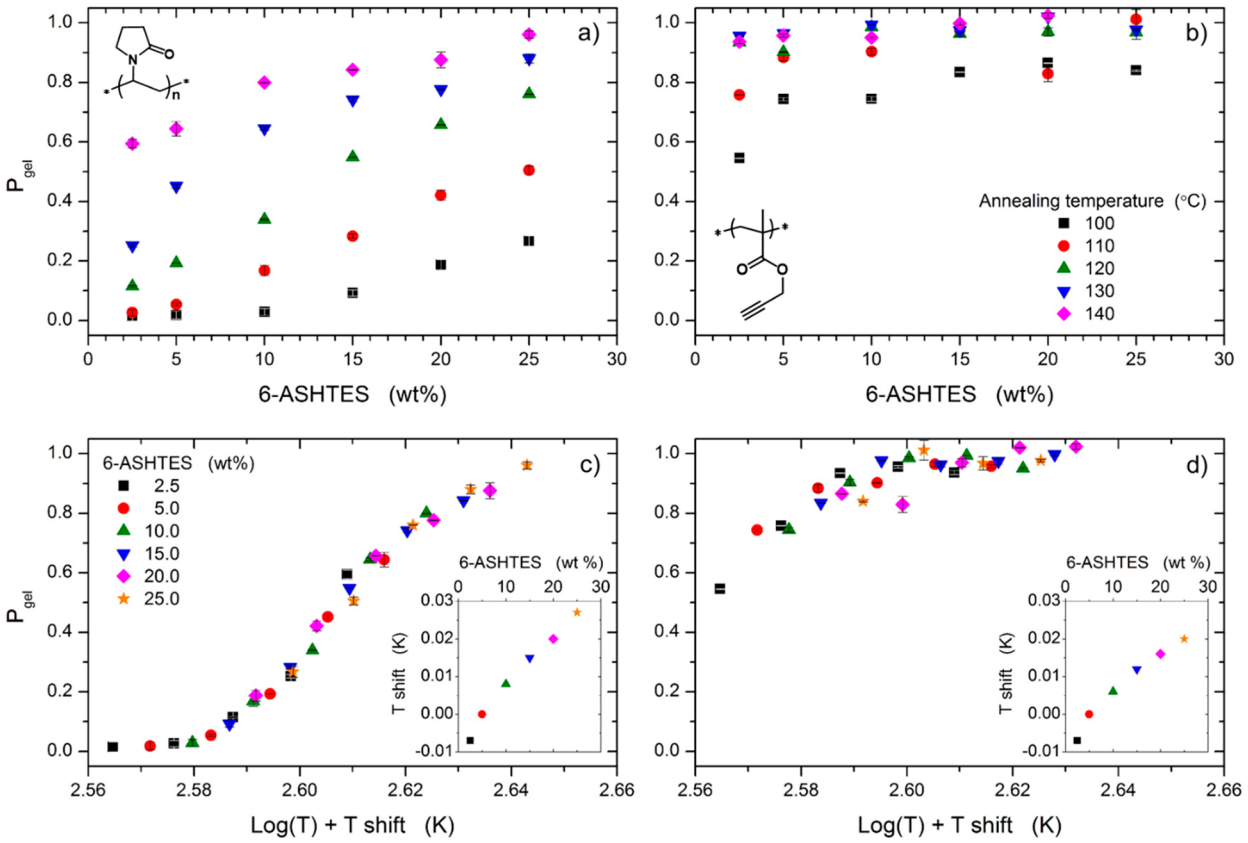

Figure 2. Gel fraction (P_{gel}) of PVP (a) and PPGMA (b) networks as a function of 6-ASHTES wt %. P_{gel} of PVP (c) and PPGMA (d) as a function of logarithm of annealing temperature (K). All samples were cross-linked by annealing at a stated temperature for 300 min.

data along the log(T) scale to make them collapse onto a master plot while recording the corresponding shifts in log(T) (i.e., T shift). Figures 2c and 2d display master plots for P_{gel} vs log(T) for PVP and PPGMA networks, respectively, cross-linked for 300 min with various amounts of 6-ASHTES at different annealing temperatures. The insets plot the temperature shift needed to collapse all data for each polymer on a master curve against the concentraton of 6-ASHTES in the original polymer/6-ASHTES mixture. The master plots in Figures 2c and 2d are both "sigmoidal-like" in shape. Importantly, the similar dependence of the T shift on the concentration of 6-ASHTES for both PVP and PPGMA (see the insets to Figures 2c and 2d) implies that the temperature dependence of the sulfamidation reaction is analogous for both PVP and PPGMA. 6-ASHTES acts both as a cross-linker and substrate-anchoring agent. The silicone headgroup condenses with hydroxyls present on the substrate and/or a silicone headgroup of another molecule in bulk (see the Supporting Information for discussion). The former leads to the covalent attachment of 6-ASHTES moieties to the substrate surface, while the latter generates intermolecular cross-links among 6-ASHTES (i.e., bulk Si−O−Si bonds). Such reactions occur readily under ambient conditions due to the presence of a minute amount of water (see the Supporting Information).[19] We reason that 6-ASHTES forms complexes featuring two (or more) 6-ASHTES molecules when the mixture is first formed while the sulfonyl azide (SAz) groups react with the polymer to form sulfonamide bonds (and it is independent of subsequent annealing).[10−12] We also note that there will be an upper limit for the concentration of 6-ASHTES above which the current method will not work. This is determined by the miscibility of the silane and the polymer in the solution that is used to cast the film. This miscibility limit depends on the polymer and the casting solvent. We have not explored this upper limit systematically, but we noted that solutions having 50 wt % of 6-ASHTES started to exhibit phase separation (data not shown).

Gel Kinetics of PVP. We investigated gel kinetics of PVP at various 6-ASHTES concentrations (5, 10, and 20 wt %) and temperatures (100, 120, and 140 °C) as a function of annealing time. The data plotted in Figure 3 reveal that P_{gel} increases with increasing the 6-ASHTES content, higher

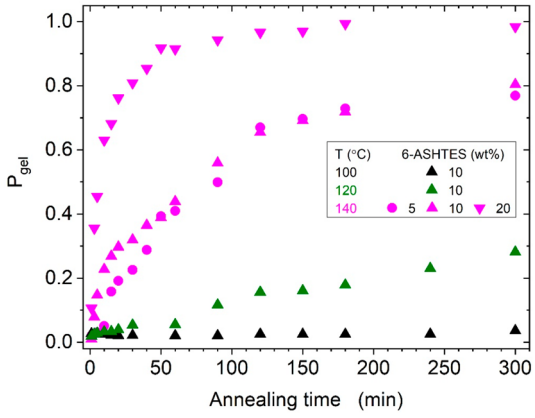

Figure 3. Gel fraction of PVP as a function of time at various temperatures (100, 120, and 140 °C) and 6-ASHTES concentrations (5, 10, and 20 wt %).

DOI: 10.1021/acs.macromol.8b02194
Macromolecules 2019, 52, 700−707

annealing temperature, and longer annealing time. Consider, for instance, networks prepared by mixing PVP with 10 wt % 6-ASHTES. Raising the annealing temperature from 100 to 140 °C increases P_{gel} for the network dramatically. Note, in particular, the rapid increase in P_{gel} when increasing the annealing temperature from 120 to 140 °C. This is fully consistent with the data plotted in Figure 5 (inset) and the corresponding discussion that confirms that P_{gel} is governed primarily by the thermal decomposition of SAz. The layers cross-linked at 100 °C form gels with low P_{gel} because 6-ASHTES reacts slowly within the time interval we investigated. The sample cross-linked at 120 °C begins to form a gel after ~60 min and reaches $P_{gel} \approx 0.30$ after annealing for 5 h, resulting in a loosely cross-linked gel. Annealing the samples for longer times would likely further increase P_{gel}. Samples annealed at 140 °C exhibit the fastest gel formation kinetics. As apparent from the data in Figure 3, the rate of gel formation also increases with increasing the concentration of 6-ASHTES in the polymer/SAz silane mixture. We have previously documented (cf. Figure 2) the correlation between the concentration of 6-ASHTES in the polymer/silane mixture and the annealing temperature in producing networks with the same P_{gel}.

On the basis of the data in Figure 3, we further postulate that, in addition to 6-ASHTES concentration and annealing temperature, the annealing time also represents a critical processing parameter that governs the structure of the final polymer network. Hence, we expect that there will be a universal "time−temperature−concentration" equivalency, similar to time−temperature superposition in polymer physics,[25,26] that governs the properties of gels formed by this method before the maximum gel point has been reached. While we currently do not have enough experimental data to verify this hypothesis, we plan to explore this further in our future work.

Influence of Chemical Structure on 6-ASHTES Thermal Cross-Linking. To explore the effect of polymer structure on the cross-linking process, we studied gel kinetics of a few additional polymers, i.e., PDMAEMA, PPGMA, and P(DMAEMA$_{0.5}$-*co*-PGMA$_{0.5}$). A thin layer of precursor polymer solution comprising a mixture of 6-ASHTES (~10 wt % in THF) and the respective polymer was deposited onto the silicon wafer and cross-linked at 140 °C for various times. From the data in Figure 4, which plots P_{gel} vs the annealing time, P_{gel} increases rapidly with increasing annealing time and reaches maximum gelation after a certain annealing time. At 300 min nearly all polymers, whose P_{gel} values are plotted in Figure 4, have reached their maximum P_{gel}. First, we compare the gel-forming behavior of PDMAEMA and PPGMA homopolymers. Both possess identical methacrylic backbone structure, but their side chains are different; i.e., PDMAEMA comprises oxyethylene and dimethyl groups (−O−CH$_2$−CH$_2$−N−(CH$_3$)$_2$), whereas PPGMA contains oxymethylene and methine groups (−O−CH$_2$−C≡CH). The additional C−H bonds in PDMAEMA (i.e., oxyethylene and two methyl groups) pendant chain enhance the probability of proton abstraction and/or C−H insertion reactions, and thus it cross-links much faster than PPGMA. The gelation behavior of P(DMAEMA$_{0.5}$-*co*-PGMA$_{0.5}$) is intermediate between those of the corresponding homopolymers, as expected.

We also studied cross-linking reactions involving zwitterionic z-P(DMAEMA$_{0.5}$-*co*-PGMA$_{0.5}$) and noticed that its gel formation is slower and yields a lower P_{gel} (≈0.79) than that

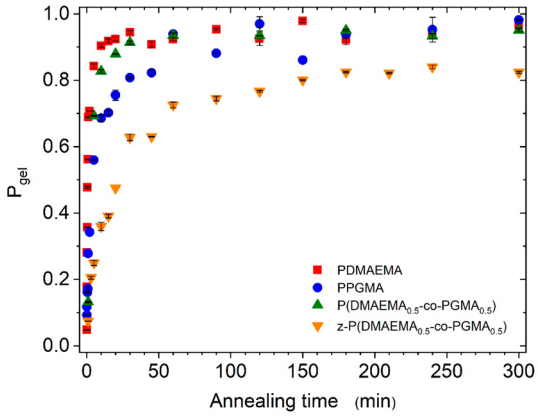

Figure 4. Gel fraction (P_{gel}) of surface-attached poly(DMAEMA), poly(PGMA), poly(DMAEMA$_{0.5}$-*co*-PGMA$_{0.5}$), z-poly-(DMAEMA$_{0.5}$-*co*-PGMA$_{0.5}$) networks. The synthesis of all polymers is detailed in the Experimental section.

recorded for the parent polymers, i.e., PDMAEMA, PPGMA, and P(DMAEMA$_{0.5}$-*co*-PGMA$_{0.5}$) ($P_{gel} \approx 0.96-0.98$). A couple of effects are likely responsible for this behavior, including the presence of bulky groups near the quaternary ammonium (R_4N^+) center and possible formation of inter- and/or intramolecular complexes between R_4N^+ and sulfonate (SO_3^-) groups of two zwitterionic units. Those lower the cross-linking rate due to the complexity associated with proton abstraction and/or C−H insertion in the aforementioned reaction centers. The side-chain structure and the presence of charges play a vital role in 6-ASHTES mediated cross-linking. The proton abstraction and/or C−H insertion reactions occur preferentially at the sp^3-hybridized C−H bonds relative to the sp or cyclic sp^2 C−H bonds. Therefore, the efficacy of the 6-ASHTES cross-linking reaction is PDMAEMA > P-(DMAEMA$_{0.5}$-*co*-PGMA$_{0.5}$) > PPGMA > z-P(DMAEMA$_{0.5}$-*co*-PGMA$_{0.5}$).

Swelling Behavior of Various Surface-Attached Network Coatings. We studied swelling characteristics of the surface-attached networks in deionized water, phosphate buffer saline (PBS) solution (pH 7.4), and methanol. We define a swelling ratio of the polymer network in a given solvent, $\alpha^{solvent}$ by eq 2:

$$\alpha^{solvent} = \frac{d^{solvent}}{d} \tag{2}$$

where d is the dry thickness of PVP gel and $d^{solvent}$ is the thickness of the same gel layer after swelling in a given solvent. The swelling ratio of the coatings was determined using Eq. 1, and the values are listed in Table 1. Hydrophilic PVP coatings exhibit high swelling by a factor of ~3.5 in water and ~3.6 in PBS. The polar amide groups in PVP interact with water

Table 1. Gel Fraction (P_{gel}) and Swelling Ratio (α) of Surface-Attached Networks Generated Using 6-ASHTES

polymer	P_{gel}	α^{water}	α^{PBS}	α^{MeOH}
PVP	0.80	3.42	3.62	3.78
PDMAEMA	0.96	1.33	1.385	1.22
P(DMAEMA$_{0.5}$-*co*-PGMA$_{0.5}$)	0.98	1.07	1.35	1.10
z-P(DMAEMA$_{0.5}$-*co*-PGMA$_{0.5}$)	0.79	1.82	2.41	1.0
PPGMA	0.98	1.0	1.0	1.0

DOI: 10.1021/acs.macromol.8b02194
Macromolecules 2019, 52, 700−707

through hydrogen bonding and cause the network strands to expand.[11,12] The hydrophobic PPGMA displays no swelling in water or PBS. Interestingly, PDMAEMA swells by a factor of 1.33 in water and 1.38 in PBS, indicating that it is moderately hydrophilic, and film swelling is driven by the partial pH-induced positive charges present on the nitrogen atom. Overall, swelling in water/PBS decreases as the hydrophobicity of the gels increases, i.e., $\alpha_{PVP} > \alpha_{z\text{-}P(DMAEMA\text{-}co\text{-}PGMA)} > \alpha_{PDMAEMA} > \alpha_{P(DMAEMA\text{-}co\text{-}PGMA)} > \alpha_{PPGMA}$, revealing that the degree of swelling is strongly influenced by even minimal changes in the molecular structure or polarity of the gels.

Uncharged PVP surface-anchored gels swell in water more than charged zwitterionic z-P($DMAEMA_{0.5}$-*co*-$PGMA_{0.5}$) networks (cf. Table 1). When the charged SO_3^- and R_4N^+ groups are solvated, the electrostatic association between opposite charges may lead to the formation of ionic bridges, which act as additional cross-linking points that suppress network swelling.[10,11] Such ionic bridges can be broken (at least partly) by changing the ionic strength of the solution. Hence, z-P($DMAEMA_{0.5}$-*co*-$PGMA_{0.5}$) networks swell more in PBS than in water because the presence of salt (i.e., mono- and disodium phosphates) in PBS screens the zwitterionic charge in sulfobetaines and may break up the ionic bridges among SO_3^- and R_4N^+ groups, causing the network strands to exert additional stretching and consequent network swelling. Additionally, the high content of hydrophobic PGMA units in z-P($DMAEMA_{0.5}$-*co*-$PGMA_{0.5}$ also contributes to lower degree of swelling in water relative to PVP. We also tested swelling of the networks in methanol. The neutral PVP displayed strong swelling (α^{MeOH} = 3.8), while the rest of the gels exhibited either weak or no swelling at all (α^{MeOH} = 1.0–1.2). This is because PDMAEMA and P($DMAEMA_{0.5}$-*co*-$PGMA_{0.5}$) contain partial positive charge on the DMAEMA units that does not favor polymer/methanol interactions,[27] and thereby not much swelling occurs. Such an effect is even more pronounced in the case of z-P($DMAEMA_{0.5}$-*co*-$PGMA_{0.5}$) networks as their zwitterionic polymeric chains tend to collapse when exposed to methanol. We note that these surface-attached network layers exhibit anisotropic (i.e., 1-dimensional) swelling in contrast to isotropic (i.e., 3-dimensional) swelling typical for bulk gels.[11,12]

DISCUSSION

The reaction between SAz and polymer is not straightforward to assess (see discussion in the Supporting Information). We can, however, monitor the activation of the azide group in 6-ASHTES at elevated temperatures using attenuated total internal reflection–Fourier transform infrared (ATR-FTIR) spectroscopy, $f^*_{6\text{-ASHTES}}$ (see Figure S3). The number of sulfonamide links is then given by $f^*_{6\text{-ASHTES}} \cdot n_{6\text{-ASHTES},0} \cdot \theta$, where $n_{6\text{-ASHTES},0}$ is the initial concentration of 6-ASHTES in the polymer/silane mixture and θ is a proportionality constant (<0.5). The value of 0.5 arises because at least two 6-ASHTES molecules are needed to form a single cross-link point in the network. θ combines multiple system parameters, i.e., the functionality of the 6-ASHTES cluster based on the number of siloxane headgroups, the efficacy of reacting the activated SAz groups with C–H bonds in the polymer, and so forth. Overall, we expect θ, whose molecular interpretation is yet to be determined through future work, to be constant for a given annealing temperature. Following this treatment, we rationalize the cross-linking reactions by plotting P_{gel} as a function of the ratio of the concentration of activated 6-ASHTES relative to the initial concentration of VP ($f^*_{6\text{-ASHTES}} \cdot n_{6\text{-ASHTES},0}/n_{VP,0}$) for networks prepared at different annealing temperatures for 300 min, as shown in Figure 5. The values of $n_{6\text{-ASHTES},0}$ and $n_{VP,0}$ are given in Table S2.

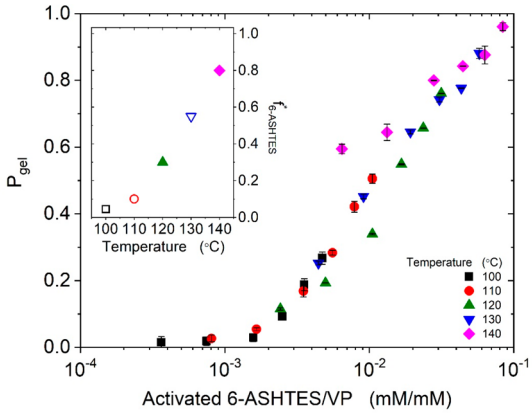

Figure 5. Gel fraction in PVP network (P_{gel}) plotted as a function of the ratio of the concentration of 6-ASHTES molecules relative to the initial concentration of VP units for networks prepared at different annealing temperatures for 300 min. The concentration of activated 6-ASHTES groups is obtained by multiplying the initial concentration of 6-ASHTES in the polymer/silane mixture (cf. Table S2) by the fraction of activated 6-ASHTES groups, $f^*_{6\text{-ASHTES}}$, given in the inset as a function of annealing temperature. The solid data in the inset have been obtained directly from the ATR-FTIR experiments (cf. Figure S3); the open symbols have been determined by fitting.

The inset to Figure 5 plots the dependence of $f^*_{6\text{-ASHTES}}$ on annealing temperature for a reaction time of 300 min. The solid symbols correspond to the data in Figure S3 ($f^*_{6\text{-ASHTES}}$ at 300 min), and the open symbols have been fitted to make all data in Figure 5 collapse onto a master plot. The $f^*_{6\text{-ASHTES}}$ values used make physical sense as their dependence on temperature coincides with the master plot in Figure 2 (i.e., P_{gel} vs $\log(T) + T$ shift). For instance, the inflection point for the data in Figure 2 occurs at $T \approx 130$ °C, which is close to the inflection point in the inset to Figure 5. In the Supporting Information we provide the same dependence of P_{gel} on the amount of activated 6-ASHTES relative to the amount of PVP in the initial mixture for another data set. (The experiments were performed using the same batch of 6-ASHTES 6 months apart during which some agglomeration among 6-ASHTES has likely occurred.) The data plotted in Figure S5 also collapse onto a master plot. This confirms that the network properties can be conveniently adjusted by tailoring the amounts of polymer and the 6-ASHTES gelator and the reaction conditions.

We compare gel swelling in networks formed from 6-ASHTES/PVP mixtures with a variable content of 6-ASHTES and PVP and annealed at different temperatures. In Figure 6, α^{water} decreases with increasing P_{gel}, as expected.[10] Importantly, the fact that (within data scatter) a unique value of α^{water} corresponds to a single value of P_{gel} further supports the notion that the overall network cross-link density (and thus gel swelling) can be tuned by varying the concentration of 6-ASHTES and PVP units in the film and the annealing temperature.

DOI: 10.1021/acs.macromol.8b02194
Macromolecules 2019, 52, 700–707

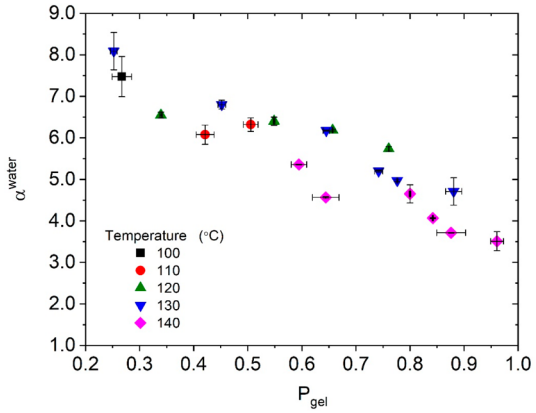

Figure 6. Swelling ratio of PVP networks (α^{water}) in water as a function of gel fraction (P_{gel}). The different symbols correspond to gels formed by cross-linking 6-ASHTES/PVP mixtures at different annealing temperatures for 300 min. The error bars were obtained by averaging data from two to three different sets.

CONCLUSION

In summary, we present a versatile one-step synthesis of surface-attached polymer networks generated by using 6-ASHTES as a cross-linker and a substrate anchoring agent. Systematic investigation of gel kinetics reveals that the cross-linking depends on the concentration of 6-ASHTES, annealing time, annealing temperature, and molecular structure of the parent polymer. In principle, any common polymer can be cross-linked and anchored onto any substrate (see Table S3) using this method as long as either of them contains C−H bonds or −OH functionalities in their structures and can be annealed at elevated temperatures (≥100 °C). This simple and robust method provides a useful new route to generate functional coatings for many practical applications.

EXPERIMENTAL SECTION

Materials. Azobis(isobutyronitrile) (AIBN), *N*,*N*-dimethylaminoethyl methacrylate (DMAEMA), polyvinylpyrrolidone (PVP), propargyl methacrylate (PGMA), and 1,3-propane sultone were purchased from Sigma-Aldrich (St. Louis, MO) and used without further purification. 6-Azidosulfonylhexyltriethoxysilane (6-ASHTES) was aquired from Gelest (Morrisville, PA). All solvents used were purchased from Fisher-Scientific (Pittsburgh, PA). Swelling experiments were performed using deionized (DI) water from Milli-Q purification system with the product resistivity of 10−15 MΩ·cm (Millipore, Billerica, MA). Phosphate buffer saline (PBS) powder was purchased from Sigma-Aldrich (St. Louis, MO) and dissolved in 1 L of deionized (DI) water to obtain a concentration of 0.01 M with a pH of 7.4. Polymer films were coated onto silicon wafers, purchased from Silicon Valley Microelectronics (Santa Clara, CA); orientation [100], thickness 0.5 mm, and diameter 100 mm.

Synthesis of PDMAEMA and PPGMA. 3.144 g (20 mmol) of DMAEMA or 2.483 g (20 mmol) of PGMA and 0.033 g (0.2 mmol) of AIBN were dissolved in 20 mL of *N*,*N*-dimethylacetamide (DMA), degassed under nitrogen gas for three freeze−thaw cycles. The mixture was stirred in a preheated oil bath at 70 °C for ∼16−18 h. After polymerization, DMA was evaporated using a rotavapor, and the polymer was dissolved in 20 mL of tetrahydrofuran (THF) and then precipitated in *n*-hexanes (for PDMAEMA) or methanol (for PPGMA). Precipitation was repeated twice, and the product was vacuum-dried overnight to obtain a white powder.

Synthesis of P(DMAEMA$_{0.50}$-*co*-PGMA$_{0.50}$). 1.572 g (10 mmol) of DMAEMA, 1.241 g (10 mmol) of PGMA, and 0.0328 g (0.2 mmol) of AIBN were dissolved in 20 mL of DMA and degassed under nitrogen for three freeze−thaw cycles. The mixture was stirred in a

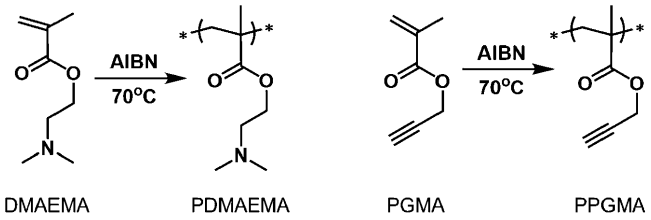

preheated oil bath at 70 °C for ∼16−18 h. After polymerization, DMA was evaporated using a rotavapor; the copolymer was dissolved in 20 mL of THF and then precipitated in *n*-hexanes. Precipitation in *n*-hexanes was repeated twice, and the product was vacuum-dried overnight to obtain a white powder.

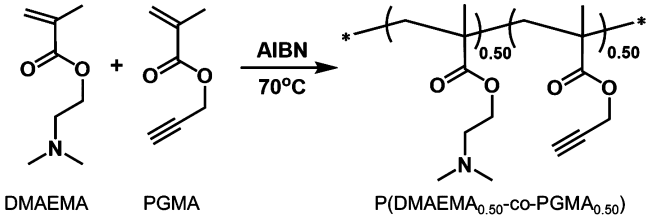

Synthesis of z-(DMAEMA$_{0.50}$-co-PGMA$_{0.50}$). 1 g (7.1 mmol) of P(DMAEMA-*co*-PGMA) was dissolved in 20 mL of trifluoroethanol (TFE); to this ∼1 g (8.1 mmol) of 1,3-propane sultone in 20 mL of TFE was added slowly for about 10 min. The reaction mixture was stirred for 24 h at room temperature. The polymer was then precipitated in *n*-hexanes 3−5 times, rinsed with TFE while filtering the polymer to remove any unreacted 1,3-propane sultone, and then vacuum-dried overnight to obtain a white powder.

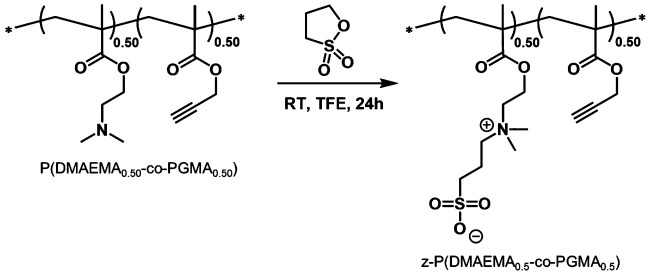

Preparation of Surface-Attached Networks. A solution containing a calculated amount of polymer (e.g., 360 mg; i.e., 90% weight fraction) and 6-ASHTES (40 mg; i.e., 10% weight fraction) was prepared with a total concentration of 20 mg/mL, i.e., 400 mg in 20 mL of a solvent (*vide infra*). The solvent was chosen based on the chemical structure of polymer; for example, we used methanol for PVP, THF for PDMAEMA, PPGMA, and P(DMAEMA$_{0.5}$-*co*-PGMA$_{0.5}$), and trifluoroethanol (TFE) for z-P(DMAEMA$_{0.5}$-*co*-PGMA$_{0.5}$). The precursor polymer solution was then deposited onto the ultraviolet/ozone (UVO)-treated silicon wafer via dip-coating (KSV NIMA single vessel dip coater) at a speed of 50 mm/min. The sample was annealed (≥100 °C) to cross-link the deposited polymer layers by using a FP82HT hot stage with a FP90 central processor (Mettler Toledo, OH). After cross-linking, the sample was thoroughly extracted in solvents from which the precursor polymer was deposited to remove any unreacted materials from the substrate surface to leave the cross-linked surface-anchored polymer networks (film thickness, $d \sim 100-200$ nm). A schematic depicting the synthesis and a scheme describing the network formation are shown in Figure 1.

Polymer Characterization. The molecular weight of the polymer (cf. Table S4) was determined using size exclusion chromatography (SEC, Wyatt Optilab rex detector along with an Alliance Waters 2695 separation module). Attenuated total internal reflection−Fourier transform infrared (ATR-FTIR) spectroscopy (Varian, USA) was used to characterize the polymer films. For each sample studied, 128

DOI: 10.1021/acs.macromol.8b02194
Macromolecules 2019, 52, 700−707

scans were collected after recording the background signal using a DTGS TEC detector with a scan resolution of 4 cm^{-1} between 600 and 4000 cm^{-1}.

Determination of Gel Fraction Using Spectroscopic Ellipsometry. The gel fraction (P_{gel}) was calculated from the change in film thickness before (d_0) and after (d) extraction of the cross-linked polymer as described in eq 1. The thickness of the polymer films was measured using variable angle spectroscopic ellipsometry (VASE, J.A. Woollam Co., USA). Reflectivity scans were collected at a 70° angle of incidence (relative to the vertical direction) in the spectral range of ($\lambda = \alpha$) 400−1000 nm in 60 steps (10 nm/step). Measurements were made on the UVO-cleaned silicon wafer deposited with the polymer. The ellipsometry data were modeled using the Fresnel formalism comprising a three-layer model in WVASE32 software (J.A. Woollam Co., version 3.682). Layer 1: Si substrate; layer 2: SiO_2 (1.5−1.7 nm thick); layer 3: polymer adlayer (refractive index modeled as a Cauchy function, $n(\lambda) = A_n + B_n/\lambda^2$, where A_n (= 1.48−1.5) and B_n (= 0.01 μm^2) are the fitting parameters).

Determination of Swelling Ratio. The swollen thickness of the film was assessed using a liquid cell adapted for spectroscopic ellipsometry. The cell was filled with ∼100 mL of solvent (water, PBS, or methanol), where the sample was immersed and allowed to reach equilibrium for ∼1−2 min. The reflectivity scans were recorded at a 70° angle of incidence across 400−1000 nm spectral range in 60 steps (10 nm/step). The swollen film thickness $d^{solvent}$ was derived directly from the effective medium approximation (EMA) based on the Fresnel formalism, and the swelling ratio $\alpha^{solvent}$ was calculated using eq 2.

■ ASSOCIATED CONTENT

Supporting Information

The Supporting Information is available free of charge on the ACS Publications website at DOI: 10.1021/acs.macromol.8b02194.

Figures S1−S5 and Tables S1−S4 (PDF)

■ AUTHOR INFORMATION

Corresponding Author

*(J.G.) E-mail: jgenzer@ncsu.edu.

ORCID

C. K. Pandiyarajan: 0000-0002-8954-9141

Jan Genzer: 0000-0002-1633-238X

Notes

The authors declare no competing financial interest.

■ ACKNOWLEDGMENTS

This work was supported in part by the NSF's Research Triangle MRSEC, DMR-1121107. Partial support from a grant DMR-1809453 is appreciated.

■ REFERENCES

(1) Forrest, S. R. The Path to Ubiquitous and Low-Cost Organic Electronic Appliances on Plastic. *Nature* **2004**, *428*, 911−918.

(2) Lei, J.-F.; Will, H. A. Thin-Film Thermocouples and Strain-Gauge Technologies for Engine Applications. *Sens. Actuators, A* **1998**, *65*, 187−193.

(3) Pandiyarajan, C. K.; Prucker, O.; Zieger, B.; Rühe, J. Influence of the Molecular Structure of Surface-Attached poly(N-Alkyl Acrylamide) Coatings on the Interaction of Surfaces with Proteins, Cells and Blood Platelets. *Macromol. Biosci.* **2013**, *13*, 873−884.

(4) Akintewe, O. O.; Dupont, S. J.; Kumar, K.; Cross, M. C.; Toomey, R. G.; Gallant, N. D. Shape-Changing Hydrogel Surfaces Trigger Rapid Release of Patterned Tissue Modules. *Acta Biomater.* **2015**, *11*, 96−103.

(5) Ionov, L.; Houbenov, N.; Sidorenko, A.; Stamm, M.; Minko, S. Smart Microfluidic Channels. *Adv. Funct. Mater.* **2006**, *16*, 1153−1160.

(6) Yang, W. J.; Neoh, K. G.; Kang, E. T.; Teo, S. L. M.; Rittschof, D. Polymer Brush Coatings for Combating Marine Biofouling. *Prog. Polym. Sci.* **2014**, *39*, 1017−1042.

(7) Zdyrko, B.; Luzinov, I. Polymer Brushes by the Grafting to Method. *Macromol. Rapid Commun.* **2011**, *32*, 859−869.

(8) Genzer, J. Surface-Bound Gradients for Studies of Soft Materials Behavior. *Annu. Rev. Mater. Res.* **2012**, *42*, 435−468.

(9) Prucker, O.; Ruhe, J. Polymer Layers through Self-Assembled Monolayers of Initiators. *Langmuir* **1998**, *14*, 6893−6898.

(10) Pandiyarajan, C. K.; Rubinstein, M.; Genzer, J. Surface-Anchored Poly(N -Isopropylacrylamide) Orthogonal Gradient Networks. *Macromolecules* **2016**, *49*, 5076−5083.

(11) Pandiyarajan, C. K.; Genzer, J. Effect of Network Density in Surface-Anchored poly(N-Isopropylacrylamide) Hydrogels on Adsorption of Fibrinogen. *Langmuir* **2017**, *33*, 1974−1983.

(12) Pandiyarajan, C. K.; Prucker, O.; Ruhe, J. Humidity Driven Swelling of the Surface-Attached Poly(N-Alkylacrylamide) Hydrogels. *Macromolecules* **2016**, *49*, 8254−8264.

(13) Li, K.; Pandiyarajan, C. K.; Prucker, O.; Rühe, J. On the Lubrication Mechanism of Surfaces Covered with Surface-Attached Hydrogels. *Macromol. Chem. Phys.* **2016**, *217*, 526−536.

(14) Navarro, R.; Pérez Perrino, M.; Prucker, O.; Rühe, J. Preparation of Surface-Attached Polymer Layers by Thermal or Photochemical Activation of α-Diazoester Moieties. *Langmuir* **2013**, *29*, 10932−10939.

(15) Wang, Y.; Yan, J.; Wang, Z.; Wu, J.; Meng, G.; Liu, Z.; Guo, X. One-Pot Fabrication of Triple-Network Structure Hydrogels with High-Strength and Self-Healing Properties. *Mater. Lett.* **2017**, *207*, 53−56.

(16) Wang, X.; Zhao, F.; Pang, B.; Qin, X.; Feng, S. Triple Network Hydrogels (TN Gels) Prepared by a One-Pot, Two-Step Method with High Mechanical Properties. *RSC Adv.* **2018**, *8*, 6789−6797.

(17) Chen, Y.; Qian, W.; Chen, R.; Zhang, H.; Li, X.; Shi, D.; Dong, W.; Chen, M.; Zhao, Y. One-Pot Preparation of Autonomously Self-Healable Elastomeric Hydrogel from Boric Acid and Random Copolymer Bearing Hydroxyl Groups. *ACS Macro Lett.* **2017**, *6*, 1129−1133.

(18) Schuh, K.; Prucker, O.; Rühe, J. Surface Attached Polymer Networks through Thermally Induced Cross-Linking of Sulfonyl Azide Group Containing Polymers. *Macromolecules* **2008**, *41*, 9284−9289.

(19) Gonzalez, L.; Rodriguez, A.; Benito, J. L. de; Marcos-Fernandez, A. Applications of an Azide Sulfonyl Silane as Elastomer Crosslinking and Coupling Agent. *J. Appl. Polym. Sci.* **1997**, *63*, 1353−1359.

(20) Pujari, S. P.; Scheres, L.; Marcelis, A. T. M.; Zuilhof, H. Covalent Surface Modification of Oxide Surfaces. *Angew. Chem., Int. Ed.* **2014**, *53*, 6322−6356.

(21) Watson, S.; Nie, M.; Wang, L.; Stokes, K. Challenges and Developments of Self-Assembled Monolayers and Polymer Brushes as a Green Lubrication Solution for Tribological Applications. *RSC Adv.* **2015**, *5*, 89698−89730.

(22) Christensen, S. K.; Chiappelli, M. C.; Hayward, R. C. Gelation of Copolymers with Pendent Benzophenone Photo-Cross-Linkers. *Macromolecules* **2012**, *45* (12), 5237−5246.

(23) Prucker, O.; Brandstetter, T.; Rühe, J. Surface-Attached Hydrogel Coatings via C,H-Insertion Crosslinking for Biomedical and Bioanalytical Applications. *Biointerphases* **2018**, *13*, 010801−010809.

(24) Körner, M.; Prucker, O.; Rühe, J. Kinetics of the Generation of Surface-Attached Polymer Networks through C, H-Insertion Reactions. *Macromolecules* **2016**, *49*, 2438−2447.

(25) Williams, M. L.; Landel, R. F.; Ferry, J. D. The Temperature Dependence of Relaxation Mechanisms in Amorphous Polymers and Other Glass-Forming Liquids. *J. Am. Chem. Soc.* **1955**, *77*, 3701−3707.

DOI: 10.1021/acs.macromol.8b02194
Macromolecules 2019, 52, 700−707

(26) Colby, R. H. Breakdown of Time-Temperature Superposition in Miscible Polymer Blends. *Polymer* **1989**, *30*, 1275−1278.
(27) Galvin, C. J.; Genzer, J. Swelling of Hydrophilic Polymer Brushes by Water and Alcohol Vapors. *Macromolecules* **2016**, *49*, 4316−4329.

DOI: 10.1021/acs.macromol.8b02194
Macromolecules 2019, 52, 700−707